NANO LETTERS

2004
Vol. 4, No. 7
1309−1312

Deformation-Free Single-Crystal Nanohelixes of Polar Nanowires

Rusen Yang, Yong Ding, and Zhong Lin Wang*

School of Materials Science and Engineering, Georgia Institute of Technology, Atlanta, Georgia 30332-0245

Received May 6, 2004; Revised Manuscript Received June 2, 2004

ABSTRACT

Ultrasmall, deformation-free, single-crystal nanohelixes/nanosprings of piezoelectric ZnO are reported. The nanohelixes are made of ∼12 nm nanowires and have a uniform mean diameter of ∼30 nm. The growth follows a hexagonal screw-coiling model, in which the growth of the nanowire is led by the Zn-terminated (0001) front surface due to self-catalysis. A sequential and periodic 60° rotation in growth direction among the six equivalent directions of $\langle 0\bar{1}11\rangle$ in an ordered and equally spaced distance results in the formation of the nanohelix. The sequential change in growth direction is to reduce the electrostatic interaction energy caused by the $\pm\{01\bar{1}1\}$ polar surfaces of the nanowire, analogous to the charge model of an RNA molecule.

Helical structures are the most fundamental structural configurations for proteins, RNAs, and other biomolecules. One-dimensional nanocoils have been observed for carbon nanotubes,[1] SiC[2] and amorphous silicon carbide.[3] The carbon coils are created due to a periodic arrangement of the paired pentagon and heptagon carbon rings in the hexagonal carbon network,[4] and the SiC coils are suggested to be formed due to the existence of planar defects and/or dislocations. Recently, we have reported nanohelixes/nanosprings,[5,6] seamless nanorings,[7] and nanobows[8] of single-crystal ZnO nanobelts, which are spontaneous polarization-induced nanostructures due to the presence of ±(0001) polar surfaces. The nanosprings have a typical diameter of ∼1−2 μm and pitch distance of ∼0.3 μm and are made of an uniformly deformed single-crystal nanobelt around the circumference. The side surfaces of the coiling nanobelt are dominated by Zn^{2+}- and O^{2-}-terminated ±(0001) surfaces with positive and negative ionic charges, respectively, creating a spontaneous polarization across the nanobelt thickness. Nanosprings are formed by rolling up single-crystal nanobelts to minimize the electrostatic energy, and their equilibrium shape and dimensions are determined by balancing the electrostatic interaction and the elastic deformation.[5,8]

In this letter, we report a new single-crystal nanohelical structure of ZnO, which is rigid and free from deformation. The nanohelixes are formed following a hexagonal screw-coiling model, analogous to the charge model of an RNA molecule. It is shown that the electrostatic interaction between the new polar surfaces of $\pm\{01\bar{1}1\}$ results in the formation of the deformation-free nanohelixes.

The ZnO nanohelixes were synthesized by thermal evaporation of a mixture of source materials consisting of powders of ZnO (0.6 g) Li_2CO_3 (0.3 g) and Ga_2O_3 (0.1 g), which were placed at the center of an alumina tube that was inserted in a horizontal tube furnace, where the temperature, pressure, and evaporation time were controlled. The tube furnace was heated to 1000 °C at a heating rate of 30 °C/min and held at the peak temperature for 2 h, which is important for controlling the growth kinetics and the formation of helical nanostructure. The tube chamber pressure was kept at 200 Torr with Ar flux at about 25 sccm (standard cubic centimeters per minute). During evaporation, the products were deposited onto an alumina substrate placed at the downstream end of the alumina tube, where the deposition temperature was 250−350 °C, which is located about 23 cm from the source material (the total length of the tube furnace is 75 cm). Our previous study[5,6] shows that the introduction of Li_2CO_3 and Ga_2O_3 in the source material makes it possible to grow polar-surface dominated nanobelts, but the mechanism is still under investigation.

The as-synthesized products were first examined by scanning electron microscopy (SEM). The high yield of the nanohelixes is manifested by the low-magnification SEM image (Figure 1a). The high-magnification SEM image (Figure 1b) clearly demonstrates the shape of the nanohelixes. Nanohelixes of both right- and left-handed chiralities have been observed at ∼50% each. With a detection limit of 1−2 at. %, energy-dispersive X-ray spectroscopy detected mainly Zn and oxygen without the presence of other elements in the sample. The observed helixes here have a typical diameter of 30 nm, which is much smaller than the ZnO nanosprings of typical diameter of 800 nm reported previously.[5]

* Corresponding author: zhong.wang@mse.gatech.edu.

10.1021/nl049317d CCC: $27.50
Published on Web 06/22/2004

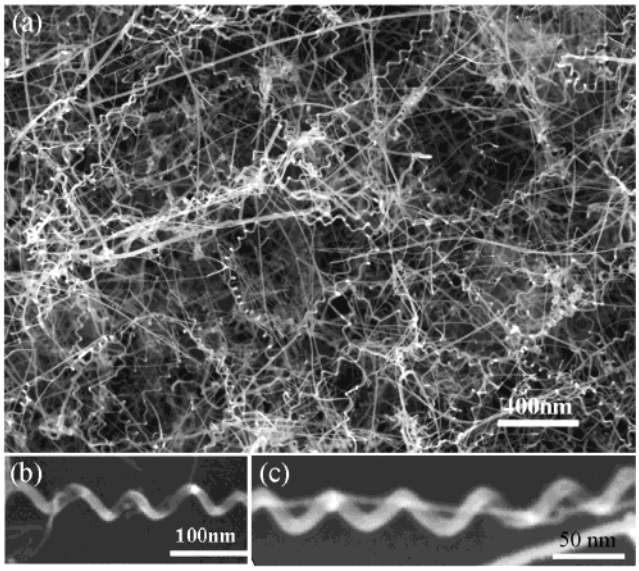

Figure 1. (a) Low-magnification SEM image of the as-synthesized nanohelixes of ZnO, showing their uniform sizes and high yield. (b) An enlarged right-handed nanohelix. (c) A small nanohelix with pitch distance of 60 nm and radius 40 nm, which grows around a straight nanowire.

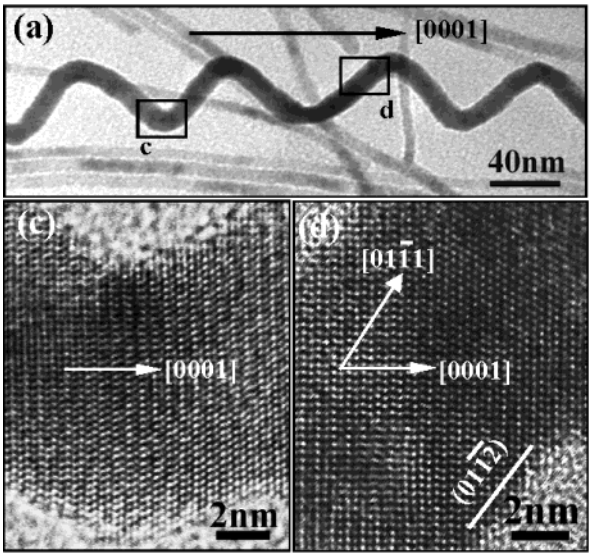

Figure 2. (a) A bright-field TEM image of a nanohelix. No significant strain contrast is found (apart from the overlap effect between the nanohelix and nanowires). (c, d) HRTEM images recorded from the c and d areas labeled in (a), respectively, showing the growth direction, side surfaces, and dislocation-free volume.

The intrinsic crystal structure of the nanohelixes has been investigated by transmission electron microscopy (TEM), showing a uniform shape and contrast (Figure 2a). High-resolution TEM (HRTEM) imaging reveals that the nanohelix has an axial direction of [0001], although the growth direction of the nanowire changes periodically along the length. Detailed HRTEM images from the regions labeled *c* and *d* in Figure 2a are displayed in Figure 2c,d, respectively, which show that the nanowire that constructs the nanohelix grows along [01$\bar{1}$1]. Because the incident electron beam is parallel to [2$\bar{1}\bar{1}$0], the two side surfaces of the nanowire are ±(01$\bar{1}\bar{2}$). No dislocations were found in the nanohelixes. It is important

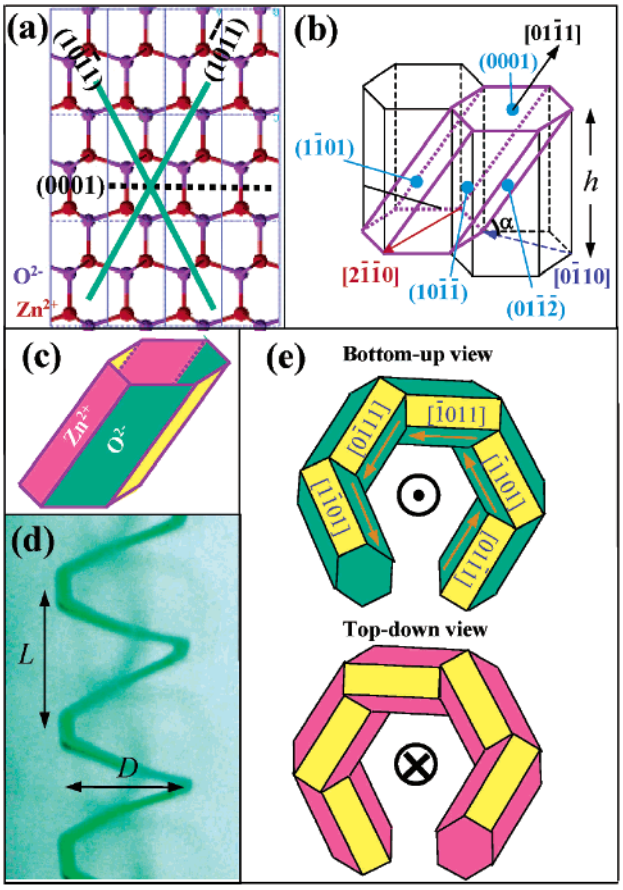

Figure 3. (a) Atomic structure of wurtzite ZnO projected along [1$\bar{2}$10], showing ±(0001), {10$\bar{1}\bar{1}$} type polar surfaces. (b) The fundamental building block of the nanowire (in purple) for constructing the nanohelixes, and its growth direction and surfaces. (c) The Zn- and O-terminated surfaces for the building block as represented by red and green colors, respectively. (d) A schematic model of the nanohelical structure, analogous to a "slinky" with 6-fold screw-rotation symmetry, where the red and green represents the Zn and oxygen terminated surfaces, respectively. (e) The bottom-up and top-down views of the nanohelical model. The distribution of charges on the surfaces of the nanohelix is analogous to the charge model of a single RNA helix.

to note that the image recorded from the "twist" point of the nanohelix shows no change in crystal lattice (Figure 2b), and the traces of the two sides are visible, indicating the nontwisted single-crystal structure of the entire nanohelix.

The nature of the ±{10$\bar{1}\bar{1}$} and ±(01$\bar{1}\bar{2}$) planes can be understood from the atomic model of ZnO. By projecting the structure along [1$\bar{2}$10], in addition to the most typical ±(0001) polar surfaces that are terminated with Zn and oxygen, respectively, ±(10$\bar{1}\bar{1}$) and ±(10$\bar{1}$1) are also polar surfaces (Figure 3a). From the structure information provided by Figure 2, the structure of the nanowire that self-coils to form the nanohelix can be constructed (Figure 3b). The nanowire grows along [01$\bar{1}$1], the two end surfaces being ±(0001), side surfaces being nonpolar ±(01$\bar{1}\bar{2}$) (represented by yellow), Zn^{2+}-terminated (1$\bar{1}$01) and ($\bar{1}$011) (represented by red), and O^{2-}-terminated ($\bar{1}$10$\bar{1}$) and (10$\bar{1}\bar{1}$) (represented by green) surfaces (see Figure 3b,c).

The structure model presented in Figure 3c is the basic building block/segment for constructing the nanohelix via a

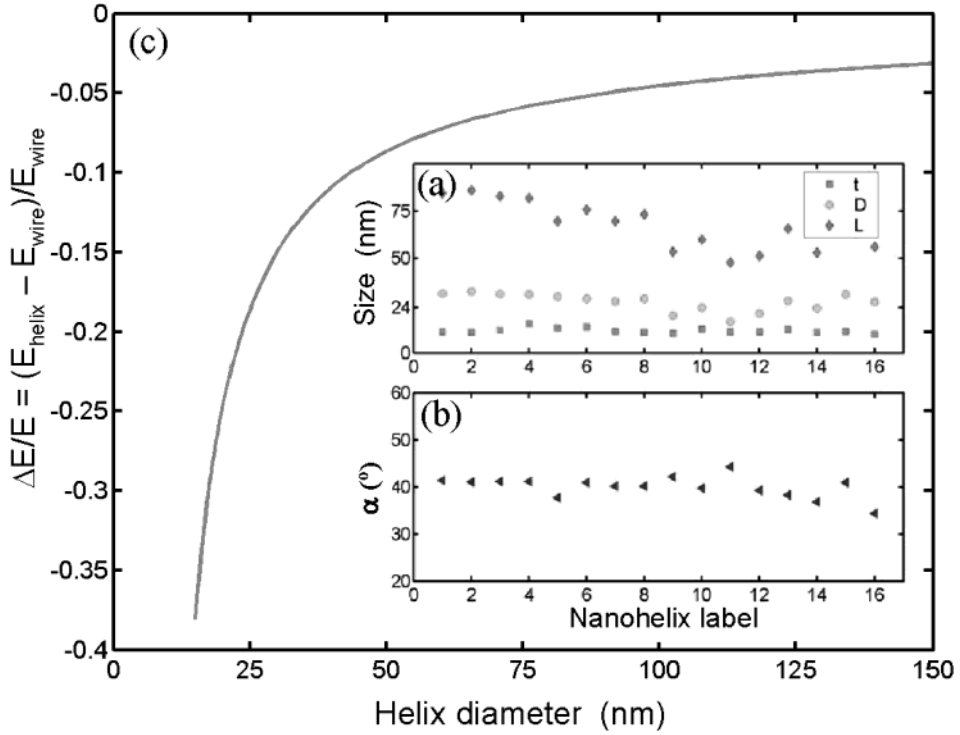

Figure 4. (a) Measured diameter (t) of the nanowire, mean diameter (D), and pitch distance (L) for a total of 16 nanohelixes. (b) The angle (see the model in Figure 3b) is derived from the experimentally measured D and L according to $\alpha = \arctan(L/3D)$. (c) Calculated change in relative electrostatic energy ($\Delta E/E$) by folding an infinitely long and straight polar nanowire into a helical structure as a function of the mean diameter, D, for $t = 11.7$ nm.

self-coiling process during the growth. Because there are a total of six crystallographically equivalent $\langle 0\bar{1}11\rangle$ directions: $[01\bar{1}1]$, $[\bar{1}101]$, $[\bar{1}011]$, $[0\bar{1}11]$, $[1\bar{1}01]$, and $[10\bar{1}1]$, and there is a 60° rotation between the two adjacent directions, thus, there are six equivalent orientations to stack the building block along the [0001] axial direction without introducing deformation or twist. A realistic three-dimensional model of the nanohelix is presented in Figure 3d, which is a stacking of the building blocks around the [0001] axis following the sequences of the six directions described above. The interface between the two building blocks is perfectly coherent and the same piece of crystal, without mismatch, translation, or twist.

The distribution of the polar charges on the surfaces of the polar nanowire is analogous to the charge model of an RNA single helix model, and it is best seen through the top and bottom views of the model (Figure 3e). If viewing the nanohelix from bottom-up, the nonpolar $(0\bar{1}12)$, Zn^{2+}-terminated $(1\bar{1}01)$ and $(\bar{1}011)$ are seen. The six growth directions of the building blocks are indicated. It is important to point out that there is no deformation introduced in the hexagonal screw-coiling stacking process, thus, no dislocations are needed to accommodate deformation. If viewing the nanohelix from top-down, the nonpolar $(0\bar{1}12)$ and the O^{2-}-terminated $(\bar{1}10\bar{1})$ and $(10\bar{1}\bar{1})$ surfaces are seen. The Zn-terminated (0001) leads the nanowire growth due to self-catalysis.[9]

The geometrical structure parameters calculated from the model shown in Figure 3b−e can be directly compared to the experimental data. If the height of the building block is h along [0001] (see Figure 3b), the pitch distance would be $L = 6h$; the mean diameter D of the nanohelix, defined as the average of the inner and outer diameters of the nanohelix and is measured between the centers of the nanowire perpendicular to the helical axis, is $D \approx 2h/\tan\alpha$, thus, $\alpha = \arctan(L/3D)$. The ZnO nanowires that coil to form helixes have uniform diameters of ~12 nm; the mean diameter D of the nanohelixes is ~30 nm (Figure 4a), but the measured pitch distance varies due to the three-dimensional projected shape in the images. The derived angle from the measured D/L is almost a constant: $\alpha \approx 40\pm2°$ (Figure 4b) and it matches well to the theoretically expected inclining angle between the nanowire growth direction $[01\bar{1}1]$ and the c-plane (0001), which is $\alpha = 42.77°$ (see Figure 3b).

To gain a quantitative understanding about the charge model proposed, we calculated the relative change in electrostatic energy ($\Delta E/E$) by folding a straight polar nanowire into a helical structure as represented by the model in Figure 3c,d without introducing deformation (Figure 4c). A straight nanowire is approximated to be a capacitor made of two long, parallel and oppositely charged strips (width W, interplanar distance t, and uniform surface charge density $\pm\sigma$). The shape of the nanohelix is approximated to be a circular screw-coiling of the nanowire with the positively charged plate directly above the negatively charged plate, being separated by a distance of t. The potential was calculated numerically by solving the integrated form of the Poisson equation. The electrostatic energy decreases after forming a nanohelix (Figure 4c). However, the magnitude of energy decrease is significant only if the mean diameter $D < 75$ nm, strongly in favor of forming small-size helixes. For the observed value of $D = 30$ nm in our experiment,

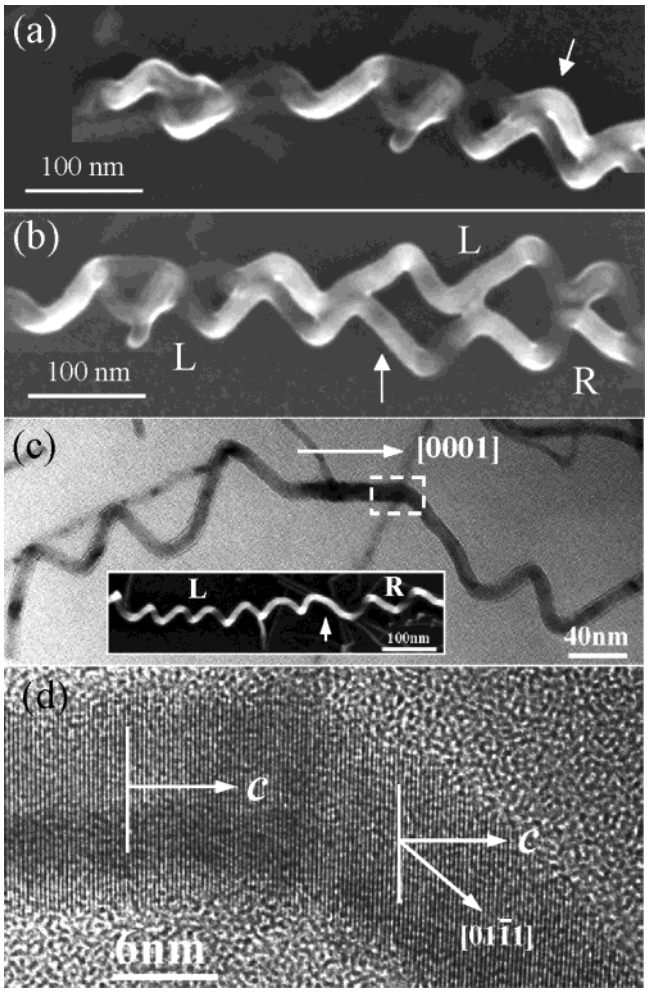

Figure 5. (a) SEM image of two nanohelixes that adhere possibly due to electrostatic attraction. (b) Two adhered nanohelixes, one of which changes its chirality from left-handed (L) to right-handed (R) through a straight segment of the nanowire. (c) TEM image of a nanohelix that changes its chirality from left-handed to right-handed, and (d) is a high-magnification TEM image from the boxed region, showing the change of growth direction from [0001] at the straight segment to [01$\bar{1}$1] in the coiled region.

$\Delta E/E = -15\%$, indicating the nanohelical structure is energetically favorable.

Switching of chirality occurs for the nanohelix. Nanohelixes that stick together have been found (see the area indicated by an arrowhead in Figure 5a). This is possible because the oppositely charged nanohelixes of the same chirality would attract each other to neutralize the interface charge. This is observed at the left-hand side of Figure 5b, where the two nanohelixes have the left-handed chirality. On the right-hand side of Figure 5b, however, one of the nanohelixes switches its chirality to right-handed, so that the two nanohelixes touch at the surface areas that have no polar charge (see the model in Figure 3e). The point at which the nanohelix changes its chirality is indicated by an arrowhead in Figure 5b. A TEM image of a nanohelix that changes its chirality during the growth is shown in Figure 5c. There is a short, straight segment of the nanowire that is along [0001], which bridges the two nanohelixes that were formed by stacking of the building blocks clockwise and counterclockwise, respectively, resulting in a change in chirality. It is important to note that the [0001] *c*-axis remains as the uniaxial direction of the entire nanostructure (see the (0002) lattice fringes in Figure 5d), and there is no twist. The result shows that the nanohelix has no preference either in left-handed or right-handed chirality. This is because the electrostatic interaction energy remains the same if the signs of the two polar surfaces are switched.

The nanohelixes reported here are distinct from the nanorings and nanosprings reported previously.[5,7,8] First, the nanohelixes are single-crystal without elastic deformation, while elastic deformation was induced in forming the nanorings and nanosprings due to the different structural configurations. Second, because no elastic/plastic deformation is introduced in forming the nanohelix, it is the electrostatic energy that dominates the entire formation process, making it possible to form the nanohelixes much smaller than the diameters of the nanorings and nanosprings. Third, the $\pm(0001)$ polar surfaces were responsible for forming the nanorings and nanosprings, while the new polar surfaces of $\pm\{01\bar{1}1\}$ are responsible for forming the nanohelixes reported here. Finally, the geometrical shape and sizes of the nanohelixes are more uniform.

We have reported a deformation-free, single-crystal nanohelical structure of ZnO and its hexagonal screw-coiling growth process. The growth of the nanowire is led by the Zn-terminated (0001) surface due to self-catalysis.[9] A sequential change in growth direction among the six equivalent growth directions of $\langle 0\bar{1}11\rangle$ in an ordered and equal distance results in the formation of the nanohelix. The entire structure is a deformation-free, block-by-block stacking process following a hexagonal screw symmetry, without introducing distortion in crystal lattices. The sequential change in growth direction is to reduce the electrostatic interaction energy between the $\pm\{01\bar{1}1\}$ polar surfaces. The structure reported here could be a potential object for studying fundamentals of nanoscale piezoelectric effect. They could have potential applications as nanoscale sensors, transducers, and actuators for applications in nanoelectromechanical systems (NEMS) and biosensing.

Acknowledgment. The work was supported by NSF NIRT ECS-0210332. Thanks to Dr. X. Y. Kong Dr. Jing Li for many stimulating discussions.

References

(1) Amelinckx, S.; Zhang, X. B.; Bernaerts, D.; Zhang, X. F.; Ivanov, V.; Nagy, J. B. *Science* **1994**, *265*, 635.
(2) Zhang, H.-F.; Wang, C.-M.; Wang, L.-S. *Nano Lett.* **2002**, *2*, 941.
(3) Zhang, D. Q.; Alkhateeb, A., Han, H.; Mahmood, H.; McIlroy, D. N. *Nano Lett.* **2003**, *3*, 983.
(4) Gao, R. P.; Wang, Z. L.; Fan, S. S. *J. Phys. Chem. B* **2000**, *104*, 1227.
(5) Kong, X. Y.; Wang, Z. L. *Nano Lett.* **2003**, *3*, 1625.
(6) Kong, X. Y.; Wang, Z. L. *Appl. Phys. Lett.* **2004**, *84*, 975.
(7) Kong, X. Y.; Ding, Y.; Yang, R. S.; Wang, Z. L. *Science* **2004**, *303*, 1348.
(8) Hughes, W. L.; Wang, Z. L. *J. Am. Chem. Soc.* **2004**, *126*, 6703.
(9) Wang, Z. L.; Kong X. Y.; Zuo, J. M. *Phys. Rev. Lett.* **2003**, *91*, 185502.

NL049317D